Preparation and Photophysics of Strongly Luminescing Cd 3 P 2 Quantum Dots

5 AUTHORS, INCLUDING:

Giersig Michael
Freie Universität Berlin
291 PUBLICATIONS **16,825** CITATIONS

SEE PROFILE

Horst Weller
University of Hamburg
391 PUBLICATIONS **27,015** CITATIONS

SEE PROFILE

Alexander Eychmüller
Technische Universität Dresden
356 PUBLICATIONS **10,800** CITATIONS

SEE PROFILE

Preparation and Photophysics of Strongly Luminescing Cd$_3$P$_2$ Quantum Dots

A. Kornowski,[†] **R. Eichberger,**[‡] **M. Giersig,**[‡] **H. Weller,**[†] **and A. Eychmüller*,**[†]

Department of Physical Chemistry, University of Hamburg, D-20146 Hamburg, Germany, and Department of Physical Chemistry, Hahn-Meitner-Institute, D-14109 Berlin, Germany

Received: November 30, 1995; In Final Form: March 15, 1996[⊗]

The wet chemical preparation, the electron microscopic characterization, and the temperature-dependent absorption as well as both the static and time-resolved fluorescence properties of Cd$_3$P$_2$ quantum dots are presented. The particles are strongly size quantized as seen from the 1.5 eV blue shift of the first electronic transition compared to the bulk bandgap of 0.5 eV. The particles emit close to the onset of absorption, exhibiting a quantum yield of 0.25 at room temperature. The luminescence decay has a multiexponential appearance at room temperature which transforms into two clearly distinguishable decay channels at low temperatures.

Introduction

In recent years research on quantum-sized semiconductor particles has expanded tremendously. This is partly due to their extraordinary photophysical properties, such as strong nonlinear optical behavior and the possibility of shifting the fundamental absorption edge of a given semiconductor material by just varying the size of the particles. Additionally, these materials hold out hopes for technological applications, such as LEDs, electrochromic devices, solar energy conversion, and even as switches in optical computers.

Progress has been made in both the synthesis and characterization of various semiconductor materials. Essentially all relevant semiconductor materials have been prepared as nanoparticles but the vast majority of the published data relates to the II−VI class of semiconductors, like CdS and CdSe. This work finds its reflection in a number of recent review articles.[1−8]

Despite some early reports on the preparation, fluorescence and photophysics of Cd$_3$P$_2$[9−11] and Cd$_3$As$_2$,[12−14] class II−V semiconductor nanocrystals have been widely disregarded.

In this article, we shall present a new preparative approach which results in an optically transparent sample of strongly size-quantized Cd$_3$P$_2$ particles suitable for temperature-dependent spectroscopic investigations. The characterization was performed using electron microscopic techniques. The longest section of the article is devoted to photophysical properties of the nanocrystals probed by temperature dependent absorption and fluorescence spectroscopy.

Experimental Section

Synthesis. In a 100 mL round-bottom flask, equipped with a septum, 10.3 mg of cadmium propionate (Strem Chemicals) was dissolved in 3 mL of *n*-propanol (p.a., Merck). To this solution 47 mL of methyl methacrylate (MMA, Aldrich, purified by standard techniques) was added followed by 45 min of bubbling with argon (saturated with MMA and propanol). To the tightly closed flask, 50 μL of triethylamine (TEA, p.a., Aldrich), which acts as a deprotonating agent and (under vigorous stirring) 1.3 mL of PH$_3$ (Messer Griesheim), was injected consecutively. After approximately 3 min the precipitation reaction was stopped by driving out the unreacted PH$_3$ with argon. The evolving solution was intensely red colored.

This solution (4 mL) together with a small amount of azobis-isobutyronitrile (p.a., Aldrich) were added to a 10 mm quartz cuvette and degassed on a vacuum line. The well-sealed sample polymerized within 3 days at room temperature under vacuum. After renewed degassing the sample was sealed off under high vacuum.

This detailed synthesis is one example out of about 100 preparations in which the Cd salts (acetate, perchlorate, 2-ethylhexanoate, acetylacetonate), the solvents (hexane, ethanol, propanol, butanol, hexanol, decanol), and the concentrations of these compounds together with the amounts of TEA and PH$_3$ injected were varied. Almost all the combinations led to particle formation, the sizes and size distributions being dependent on the exact reaction conditions. Here, we chose to describe the preparation in which an optically transparent polymer block, suitable for low-temperature spectroscopy, was obtained.

Apparatus. The technical equipment used was essentially the same as described in earlier publications.[15−17] That is, the absorption spectra were recorded with a Bruins Instruments Omega 20 photometer, while the fluorescence spectra were measured using a self-built spectrometer equipped with a sensitive photomultiplier and a germanium detector for simultaneous recording in the visible and near-infrared region, respectively. The time-resolved fluorescence was evaluated by time-correlated single-photon counting using an argon ion laser (Spectra Physics) as the excitation source and a microchannel-plate photomultiplier (Hamamatsu) as the detector. The laser was modelocked at 488 nm, and the repetition rate was reduced to 40 kHz with an external acoustooptic modulator. The temperature-dependent measurements were carried out in a Leybold VSK 4-300 continuous flow He cryostat. Electron microscopy was performed with a Phillips CM12 super twin equipped with an EDX detector for X-ray fluorescence.

Results and Discussion

Characterization. An electron microscopy image, which gives an overview of the particles prepared, is shown in Figure 1a. The histogram in Figure 1b was produced by measuring the diameters of approximately 200 particles and plotting them against their relative frequencies. From this analysis a mean diameter of 27 ± 4 Å is determined. The inset of Figure 1a shows a micrograph of a single particle at higher magnification which exhibits lattice planes at a distance of 2.1 Å. Together with electron diffraction data, from which lattice plane distances
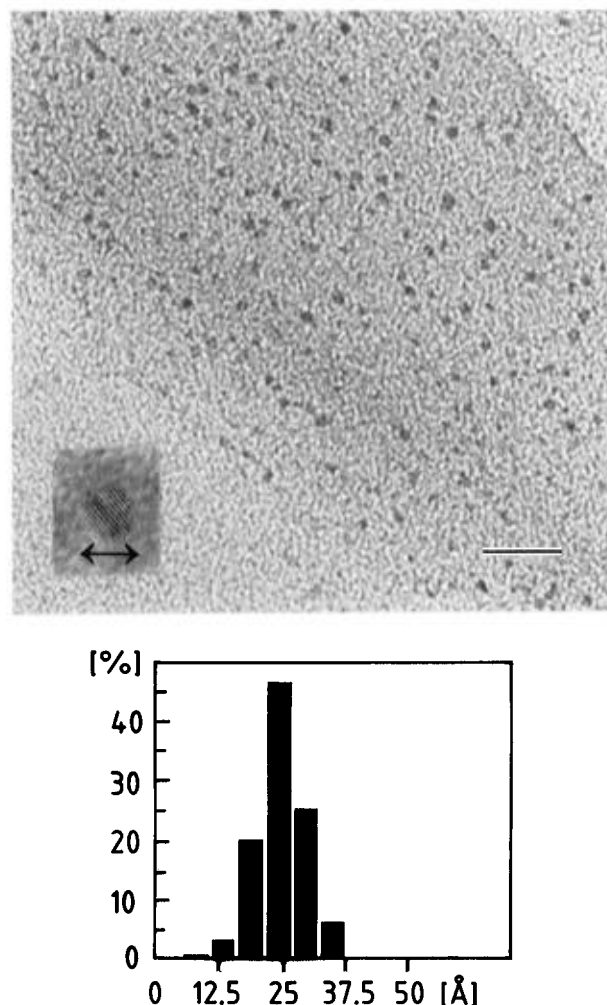
**Figure 1.** (a) Electron microscopic picture of Cd_3P_2 particles (the bar equals 220 Å). The inset shows an image of a single particle at higher resolution (the bar equals 30 Å). (b) Particle size histogram obtained from TEM images.

of 3.35, 2.9, 2.1, 1.74, and 1.28 Å were deduced, the sample prepared is undoubtedly characterized as the tetragonal phase of Cd_3P_2. The stoichiometry is also nicely reflected in the X-ray fluorescence spectra which give a Cd/P ratio of 1.49, which is in surprisingly good agreement with the summation formula. From these data a mean agglomeration number of approximately 80 (in terms of Cd_3P_2 units) or 400 atoms is derived. Considering the tetragonal unit cell these numbers correspond to roughly 10 unit cells.[18]

Photophysical Properties. The room-temperature absorption spectrum of the Cd_3P_2 particles prepared is shown in Figure 2a. It exhibits a strongly shifted first electronic transition (located at about 600 nm = 2.07 eV) compared to the bulk bandgap of Cd_3P_2 of $E_{g,direct} = 0.5$ eV.[19-21] This shift is explained in terms of quantum confinement of the photogenerated electron–hole pair (or exciton). Considering the material constants of bulk Cd_3P_2, i.e., the effective masses of the electron ($0.05\ m_0$) and the hole ($0.4\ m_0$) and the high-frequency dielectric constant (≈ 15),[22] a radius of the exciton of about 180 Å is calculated. Thus, the observed large shift of the transition energy of about 1.5 eV is consistent with the restriction of a relatively voluminous exciton in the small volume of the 27 Å particles. From a phosphorus analysis, from which the dot concentration in the sample can be determined, the remarkably high extinction coefficient of $\epsilon(600\ \text{nm}) \approx 1 \times 10^6$ L mol^{-1} cm^{-1} per dot (or 12 500 L mol^{-1} cm^{-1} referred to the analytical concentration of Cd_3P_2 molecules) is calculated. This is in
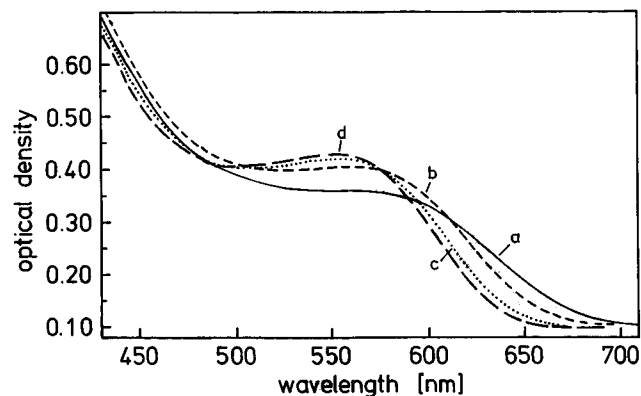
Figure 2. Absorption spectra of the Cd_3P_2 sample at different temperatures (a, 300 K; b, 206 K; c, 104 K; d, 4 K).
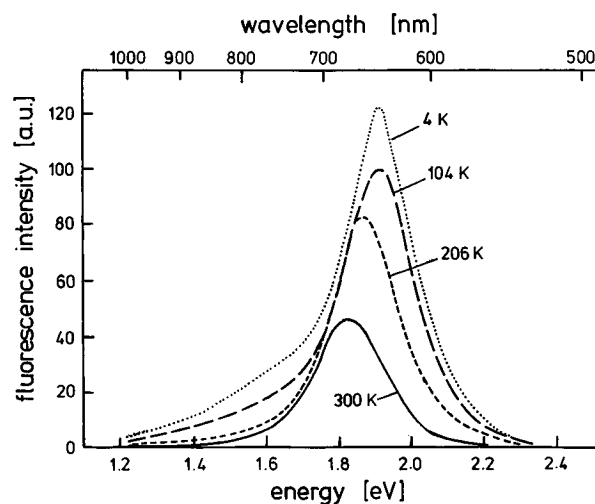

Figure 3. Fluorescence spectra taken at the same temperatures as the absorption spectra in Figure 2 ($\lambda_{exc} = 490$ nm).

accordance with the large extinction coefficients reported for CdTe and CdS particles of comparable sizes.[17,23]

The absorption spectra Figure 2b–d were taken at 206, 104, and 4 K, respectively. It can be seen that the polymer sample remains transparent and that the absorption is shifted to higher energies with decreasing temperature while the oscillator strength is conserved. The spectrum becomes a little more structured at 4 K featuring a relative maximum at about 560 nm and a relative minimum at about 500 nm. The particle size distribution is assumed to be the reason for the still relatively broad absorption; in other words, we are still facing an inhomogeneously broadened absorption spectrum.

Four fluorescence spectra, taken at the same temperatures as the absorption spectra shown in Figure 2, are depicted in Figure 3. An excitation wavelength of 490 nm was chosen, as the optical density of the sample at this wavelength is nearly temperature independent. As a consequence, the fluorescence intensities shown in Figure 3 are directly comparable. The room temperature fluorescence band is almost symmetrical with a maximum at about 675 nm (1.84 eV). The quantum yield of this fluorescence is very high. It has been calculated to be 0.25 by a careful comparison to a rhodamine 6G fluorescence dye solution emitting in the same spectral region. This is among the highest reliably determined room temperature fluorescence quantum yields of semiconductor quantum dots reported so far.[24] Obviously, the radiative recombination is able to successfully compete with radiationless transitions in the particles, the reason for which might be a relatively high activation energy for the radiationless processes (or a poor coupling to the particles'

Strongly Luminescing Cd$_3$P$_2$ Quantum Dots

J. Phys. Chem., Vol. 100, No. 30, 1996 **12469**
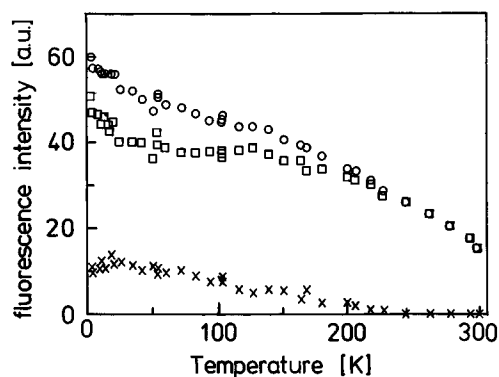
Figure 4. Fluorescence intensity as a function of temperature: total fluorescence intensity (○), short-wavelength emission (□), and long-wavelength emission (×).
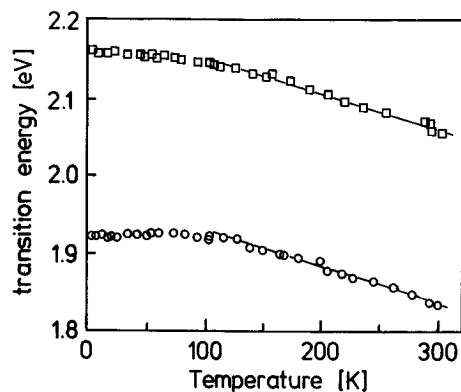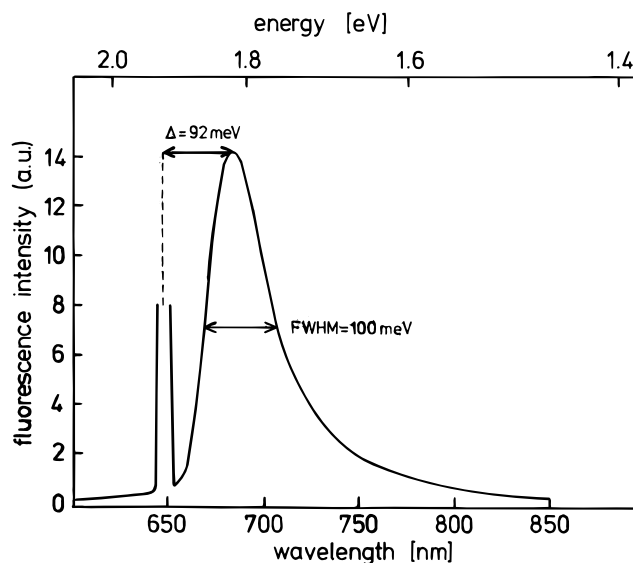

Figure 5. Fluorescence maximum (○) and energy of the first electronic transition as deduced from the absorption spectra (□) versus temperature.

Figure 6. Fluorescence spectrum taken at 20 K with an excitation wavelength of $\lambda_{exc} = 650$ nm.

phonons). The high quantum yield is even more surprising if one reflects that particles of, for example, CdS and CdSe luminesce poorly when approaching the strong confinement regime.

Returning to Figure 3, three additional features are observed with decreasing temperature: (1) the fluorescence intensity increases, (2) the fluorescence maximum shifts to higher energy, and (3) between 200 and 100 K a long-wavelength shoulder begins to evolve in the fluorescence spectra.

Observations 1 and 3 are summarized in Figure 4, where the fluorescence intensities are plotted versus temperature. The circles denote the total fluorescence intensity, the squares the intensity of the short-wavelength luminescence and the crosses the ones of the low-energy band. (The latter was roughly calculated by doubling the area under the spectra from 1.15 to 1.61 eV and subsequent subtraction from the total intensity at the respective temperature.) The total fluorescence intensity increases by approximately a factor of 4 from room temperature to 4 K, which results in a fluorescence quantum yield of 1 at the lowest temperatures. From the total fluorescence a maximum of 25% falls to the share of the long-wavelength luminescence.

The emission maximum as a function of temperature is plotted in Figure 5. The graph resembles similar data published on the temperature shift of the transition energy in CdS quantum dots of different sizes.[17] From 300 K to about 100 K a linear shift ($dE_{fl.(300\to100\ K)}/dT = -4.7 \times 10^{-4}$ eV/K) is observed, below 100 K the transition energy seems to become temperature independent. A correct deconvolution of the long-wavelength band (which tends to "draw" the fluorescence maximum to lower energies) from the total fluorescence yields a slight temperature dependence of the location of the fluorescence

maximum below 100 K (see below). As reported for the smallest CdS particles the temperature dependence in the linear region above 100 K is stronger than for the respective bulk materials.[25] This observation is still not understood which should encourage theoreticians to work on this property of size-quantized matter.

As seen in Figure 5, the shift of the transition energy, deduced from the absorption spectra, exhibits the same temperature dependence as the fluorescence maximum from 300 to 100 K, whereas below 100 K the energy increases linearly with a smaller slope of $dE_{abs(<100\ K)}/dT = -1.5 \times 10^{-4}$ eV/K, consistent with the estimate above as well as with data obtained with bulk material.[25]

Together with the observed Stokes shift, findings 1−3 are taken as indications for at least four electronic states being involved in the photophysics of Cd$_3$P$_2$ quantum dots: conduction and valence band separated by approximately 2.15 eV at 4 K and two (or more) trap states giving rise to the short- and long-wavelength luminescence bands.

The size of the Stokes shift is best seen in Figure 6. There, a fluorescence spectrum taken at 20 K is shown, where we chose 650 nm as the excitation wavelength. At this wavelength only the very biggest particles contained in the sample are excited at this temperature (cf. Figure 2) and so particle size inhomogeneities are excluded. It can be seen that the Stokes shift amounts to 92 meV. This energy difference could be interpreted as a localization energy of the exciton (i.e., the conversion from a free exciton into an exciton bound at a defect, for example). It should be noted that in work on Cd$_3$P$_2$ thin films (showing the low-temperature bulk bandgap of 0.6 eV) a Stokes shift of 100 meV, which is in the same order of magnitude as in our measurements, has been observed.[26] The authors interpret this finding as being due to a spread of donor states close to the conduction band edge. So far, we are left with the speculation that probably the tetragonal crystal structure with its cation "vacancies"[18] (which might be efficient trapping sites) is responsible for the large Stokes shift.

Also recognizable from Figure 6 (in comparison to Figure 3) is a phenomenon frequently called fluorescence line narrowing. Thus, by excitation of only the biggest particles in a distribution a fluorescence spectrum of a monodisperse sample is obtained. By this, a reduction of the fluorescence line width by a factor of more than 2 is observed resulting in a full width
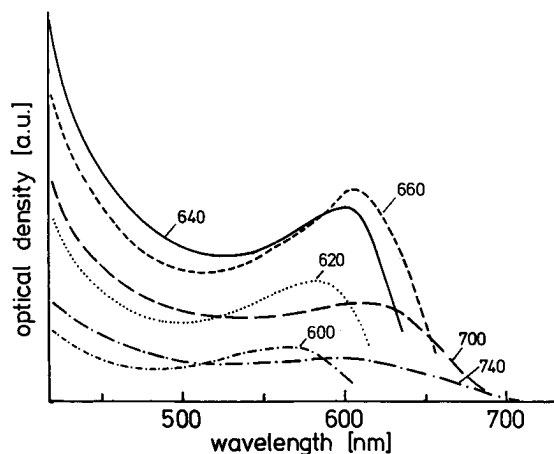
Figure 7. Fluorescence excitation spectra obtained with different observation wavelengths as indicated ($T = 206$ K).

Figure 8. Time-resolved fluorescence decay curves at different temperatures (indicated at the curves, $\lambda_{exc} = 488$ nm, $\lambda_{obs} > 530$ nm).

at half-maximum of ≈ 100 meV. This value is of the order of the fluorescence line width of very narrowly distributed CdS particles. However, in contrast to results from CdSe quantum dots of high quality, obtained by time-gated fluorescence spectroscopy,[27-29] no phonon progression is seen in the fluorescence spectra of Cd_3P_2 particles. In future work it has to be clarified whether the reason for this is of an experimental or a fundamental nature.

Another peculiarity seen in Figure 6 is the reduced long-wavelength luminescence intensity compared to the low-temperature spectrum from Figure 3 ($\lambda_{exc} = 490$ nm). Hence, it may be inferred that larger particles exhibit relatively more short wavelength luminescence and that smaller particles have the ability to additionally fluoresce at long wavelengths. This conclusion is supported by inspection of a series fluorescence excitation spectra (cf. Figure 7) taken at 206 K. The numbers on the spectra indicate the observation wavelengths. As a general trend it can be seen that the nicely developed relative maxima in the fluorescence excitation spectra occur at shorter wavelengths the shorter the observation wavelength. This is in accordance with the size quantization of the particles: the smaller the particles the higher are the transition energies of absorption and emission. This is a correct description as long as the observation wavelength is chosen to be located in the main (short wavelength) emission band. Moving the observation wavelength into the long wavelength shoulder ($\lambda_{obs} = 740$ nm) of the emission spectrum a less structured fluorescence excitation spectrum is gained showing a maximum at shorter wavelengths than expected from the size quantization alone. This is interpreted as being the result of an overlap of emission from the largest particles (close to their absorption) and small particles with a large long-wavelength fluorescence component.

As a last example of this summary of some of the photophysical properties of the Cd_3P_2 particles some luminescence decay curves taken at the temperatures indicated ($\lambda_{obs} > 530$ nm) are plotted in Figure 8. The room-temperature signal follows multiexponential decay kinetics as in all other time-resolved experiments on all the different particles reported so far. (In Cd_3P_2 single crystals two recombination channels with decay times of 30 and 100 ns, respectively, have been observed.[30]) In contrast to, for example, CdS quantum dots,[31] the dependence of the luminescence decay on temperature reveals a distinct separation into two decay channels, one with a low activation energy resulting in an almost temperature independent fluorescence decay with a lifetime of $1-2$ ns and one with a higher activation energy ending at lifetimes longer than our longest observed time window of 25 μs at the lowest
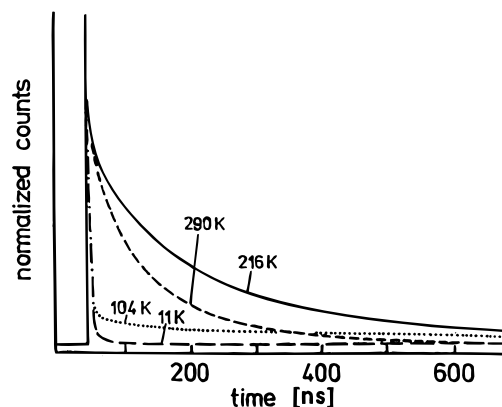
temperatures investigated. The separation into two components is best seen by comparison of the decay signals at 216 and 104 K in Figure 8. On the time scale of 600 ns shown here the slow component virtually does not decay at 104 K, whereas at higher temperature a "lifetime" of some 100 ns is observed. The fast component, however, is clearly seen at 104 K, whereas it is just one of the many lifetimes of which the decay at 216 K is composed. Although the fast component is clearly observable and separable from the overall decay at temperatures below approximately 200 K the intensity remains very minor ($<0.1\%$). A very thorough search involving different excitation and luminescence wavelengths, time scales, and temperatures did not yield a combination of these experimental parameters allowing a clear appointment to the physical origin of the two decay components observed. Thus, we are left with the surprising result that at low temperatures (almost) the whole excitation energy is quickly converted into a very slow decaying luminescence. In molecular photochemistry this would be interpreted as a fast intersystem crossing from an excited singlet state into a triplet state with the subsequent (slow) phosphorescence back into the singlet ground state. Currently, time-resolved low-temperature EPR experiments are planned to clarify whether in quantum dots similar spin-forbidden transitions are also operative.

References and Notes

(1) Henglein, A. *Chem. Rev.* **1989**, *89*, 1861.
(2) Wang, Y.; Herron, N. *J. Phys. Chem.* **1991**, *95*, 525.
(3) Brus, L. E. *Appl. Phys. A* **1991**, *53*, 465.
(4) Weller, H. *Angew. Chem., Int. Ed. Engl.* **1993**, *32*, 41.
(5) Weller, H. *Adv. Mater.* **1993**, *5*, 88.
(6) Special issue on quantum dots: *Isr. J. Chem.* **1993**, *33*.
(7) Henglein, A. *Ber. Bunsen-Ges. Phys. Chem.* **1995**, *99*, 903.
(8) Weller, H.; Eychmüller, A. *Adv. Photochem.* **1995**, *20*, 165.
(9) Weller, H.; Fojtik, A.; Henglein, A. *Chem. Phys. Lett.* **1985**, *117*, 485.
(10) Haase, M.; Weller, H.; Henglein, A. *Ber. Bunsen-Ges. Phys. Chem.* **1988**, *92*, 1103.
(11) Kietzmann, R.; Willig, F.; Weller, H.; Vogel, R.; Nath, D. N.; Eichberger, R.; Liska, P.; Lehnert, J. *Mol. Cryst. Liq. Cryst.* **1991**, *194*, 169.
(12) Fojtik, A.; Weller, H.; Henglein, A. *Chem. Phys. Lett.* **1985**, *120*, 552.
(13) Dannhauser, T.; O'Neil, M.; Johansson, K.; Whitten, D.; McLendon, G. *J. Phys. Chem.* **1986**, *90*, 6074.
(14) O'Neil, M.; Marohn, J.; McLendon, G. *J. Phys. Chem.* **1990**, *94*, 4356.
(15) Hässelbarth, A.; Eychmüller, A.; Eichberger, R.; Giersig, M.; Mews, A.; Weller, H. *J. Phys. Chem.* **1993**, *97*, 5333.

Strongly Luminescing Cd$_3$P$_2$ Quantum Dots

J. Phys. Chem., Vol. 100, No. 30, 1996 **12471**

(16) Mews, A.; Eychmüller, A.; Giersig, M.; Schooss, D.; Weller, H. *J. Phys. Chem.* **1994**, *98*, 934.

(17) Vossmeyer, T.; Katsikas, L.; Giersig, M.; Chemseddine, A.; Diesner, K.; Popovic, I. G.; Eychmüller, A.; Weller, H. *J. Phys. Chem.* **1994**, *98*, 7665.

(18) Sieranski, K.; Szatkowski, J.; Misiewicz, J. *Phys. Rev. B* **1994**, *50*, 7331.

(19) Haacke, G.; Castellion, G. A. *J. Appl. Phys.* **1964**, *35*, 2484.

(20) Bishop, S. G.; Moore, W. J.; Swiggart, E. M. *Appl. Phys. Lett.* **1969**, *15*, 12.

(21) Lin-Chung, P. J. *Phys. Status Solidi (b)* **1971**, *47*, 33.

(22) Landoldt-Börnstein; *Numerical data and Functional Relationships in Science and Technology*; Springer: Berlin, 1983; Vol. 3−17e, Sections 9.5.4.1 and 9.5.4.5.

(23) Rajh, T.; Micic, O. I.; Nozik, A. J. *J. Phys. Chem.* **1993**, *97*, 11999.

(24) Recently, a 0.5 luminescence quantum yield has been reported for ZnS on CdSe capped particles: Hines, M. A.; Guyot-Sionnest, P. *J. Phys. Chem.* **1996**, *100*, 468.

(25) Radoff, P. L.; Bishop, S. G. *Phys. Rev. B* **1972**, *5*, 442.

(26) Rao, D. R.; Nayak, A. *J. Appl. Phys.* **1993**, *74*, 214.

(27) Bawendi, M. G.; Wilson, W. L.; Rothberg, L.; Carroll, P. J.; Jedju, T. M.; Steigerwald, M. L.; Brus, L. E. *Phys. Rev. Lett.* **1990**, *65*, 1623.

(28) Bawendi, M. G.; Carroll, P. J.; Wilson, W. L.; Brus, L. E. *J. Chem. Phys.* **1992**, *96*, 946.

(29) Nirmal, M.; Murray, C. B.; Norris, D. J.; Bawendi, M. G. *Z. Phys. D* **1993**, *26*, 361.

(30) Arushanov, E. K.; Kulyuk, L. L.; Nateprov, A. N.; Radautsan, S. I.; Shemyakova, T. D.; Shtanov, A. A. *Sov. Phys. Semiconduct.* **1989**, *23*, 35.

(31) Eychmüller, A.; Hässelbarth, A.; Katsikas, L.; Weller, H. *Ber. Bunsen-Ges. Phys. Chem.* **1991**, *95*, 79.